



ORIGINAL RESEARCH

New non-contrast MRI of endolymphatic hydrops in Ménière's disease considering inversion time

Masanori Ishii MD, PhD^{1,2,3}  | Hiroshi Tanaka MD⁴ | Ryuichi Asai BS⁵ |
Yasuhisa Kanai BS⁴ | Yujin Kato MD³ | Yusuke Ito MD³ |
Fumihiko Mochizuki MD, PhD⁶ | Masami Yoneyama PhD⁷ | Gail Ishiyama MD⁸  |
Akira Ishiyama MD⁹

¹Department of Otorhinolaryngology, Japan Community Healthcare Organization (JCHO) Tokyo Shinjuku Medical Center, Tokyo, Japan

²Department of Neurotology, Advanced Imaging Center (AIC) Yaesu Clinic, Tokyo, Japan

³Department of Otorhinolaryngology, The Jikei University School of Medicine, Tokyo, Japan

⁴Department of Radiology, Ochanomizu Surugadai Clinic, Tokyo, Japan

⁵Department of Radiology, Advanced Imaging Center (AIC) Yaesu Clinic, Tokyo, Japan

⁶Department of Otolaryngology, University of Miami Miller School of Medicine, Miami, Florida, USA

⁷MR Clinical Science, Philips, Japan

⁸Department of Neurology, David Geffen School of Medicine at UCLA, Los Angeles, California, USA

⁹Department of Head & Neck Surgery, David Geffen School of Medicine at UCLA, Los Angeles, California, USA

Correspondence

Masanori Ishii, Department of
Otorhinolaryngology, Tokyo Shinjuku Medical
Center, 5-1, Tsukudo-chou, Shinjyuku-ku,
Tokyo 162-8543, Japan.
Email: dr.mishii@gmail.com

Abstract

Objectives: Three-tesla MRI with gadolinium-based contrast agents is important in diagnosing Ménière's disease. However, contrast agents cannot be used in some patients. By using the compositional difference between the inner ear endolymph and perilymph, we performed basic and clinical research focused on potassium ions and protein to find the optimal parameters for visualizing endolymphatic hydrops on MRI without contrast. We then examined the relationship between severity stage and visualization rate of endolymphatic hydrops.

Methods: In phantom experiments simulating the endolymph and perilymph, we explored MRI parameters that could be used to separate endolymph from perilymph by gradually changing the inversion time. We then used these parameters to perform both new non-contrast MRI and contrast MRI on the same day in Ménière's disease patients, and we compared the visualization rates of endolymphatic hydrops under the two modalities. Fifty patients were selected from 478 patients with Ménière's disease of different severity stages; 12 patients had asthma and allergy to contrast agents.

Meeting information: The annual meeting of Japanese Society of Otorhinolaryngology-Head and Neck Surgery, Fukuoka, Japan, May 19, 2023, and the annual meeting of Japan Society for Equilibrium Research, Niigata Japan, October 27, 2023.

This is an open access article under the terms of the [Creative Commons Attribution-NonCommercial-NoDerivs](https://creativecommons.org/licenses/by-nc-nd/4.0/) License, which permits use and distribution in any medium, provided the original work is properly cited, the use is non-commercial and no modifications or adaptations are made.

© 2024 The Author(s). *Laryngoscope Investigative Otolaryngology* published by Wiley Periodicals LLC on behalf of The Triological Society.

Results: The higher the disease stage, the higher the endolymphatic hydrops visualization rate. The new non-contrast MRI gave significantly higher ($p < .01$) visualization rates of endolymphatic hydrops on the affected side in patients at Stage 3 or above than in Stages 1 and 2 combined.

Conclusion: New non-contrast MRI with parameters focusing on the endolymph-perilymph difference in the density of protons surrounding the potassium ions and protein can produce images consistent with endolymphatic hydrops. We believe that this groundbreaking method will be useful for diagnosing Ménière's disease in patients.

Evidence Level: Clinical studies are at evidence level 3 in non-randomized controlled trials.

KEYWORDS

endolymphatic hydrops, inversion recovery (RI), inversion time (TI), Ménière's disease, non-contrast MRI

1 | INTRODUCTION

Ménière's disease is an important inner ear disorder characterized by sudden attacks of vertigo and hearing loss. With increasing severity of the disease, hearing loss, tinnitus, and vertigo attacks impose substantial burdens, not only on patients' personal lives but also on their social lives. Therefore, correct diagnosis of severe disease is extremely important. Ménière's disease was first reported as an inner ear disease in 1861 by Ménière.¹ Hallpike and Cairns² and Yamakawa³ reported in 1938 that the pathological feature of the disease was endolymphatic hydrops. According to the 1995 diagnostic criteria for Ménière's disease of the AAO-HNS (Committee on Hearing and Equilibrium of the American Academy of Otolaryngology—Head and Neck Surgery), a definitive diagnosis of Ménière's disease was made when post-mortem examination of the temporal bone revealed endolymphatic hydrops.⁴ However, the 2015 AAO-HNS criteria for Ménière's disease deleted the pathological confirmation.⁵ The 2015 international diagnostic criteria jointly formulated by several organizations, including the Bárány Society, state that endolymphatic hydrops is frequently observed in Ménière's disease, both pathologically and on contrast-enhanced magnetic resonance imaging (MRI).⁶

In 2007, Nakashima et al. succeeded in detecting endolymphatic hydrops by MRI by injecting a gadolinium-based contrast agent (GBCA) into the middle ear cavity by tympanocentesis and imaging the inner ear the following day.⁷ However, this method had disadvantages, including complications such as otitis media, sequelae such as tympanic membrane perforation, and a long-time interval of 24 h between the injection of a GBCA into the middle ear cavity and imaging.

In 2012, Naganawa et al. successfully obtained clear images of endolymphatic hydrops by MRI of the inner ear 4 h after intravenous administration of a GBCA.⁸ The images were obtained by subtracting a positive endolymph image (PEI) from a positive perilymph image (PPI) by using 3D FLAIR (three-dimensional fluid-attenuated inversion recovery).⁹ This method, which creates a HYDROPS (HYbriD of Reversed image Of Positive endolymph signal and native image of

positive perilymph Signal), is an excellent diagnostic technique.^{8,9} The method was reported to be very important for understanding the pathogenesis of Ménière's disease¹⁰ and is now valued highly. Detection of endolymphatic hydrops on contrast-enhanced MRI is one of the diagnostic criteria for definitive Ménière's disease in Japan.¹¹ However, contrast MRI is generally contraindicated in patients with allergies to contrast agents or with bronchial asthma or renal insufficiency, and these patients therefore cannot undergo this procedure.

The dynamic hydration numbers of potassium ions range from 6 to 8, according to an analysis using nuclear magnetic resonance spectroscopy.¹² These numbers are very close to those from analyses using X-ray diffraction or Monte Carlo simulations.^{12,13} This means that there are many protons that form water molecules around the K^+ ions. The K^+ concentrations differ markedly between the endolymph and the perilymph: the K^+ concentration of the endolymph is high, at about 150 mEq/L,¹⁴ whereas that of the perilymph is quite low, at about 5 to 9 mEq/L.¹⁵ The concentration of protein is 20 to 30 mg/dL in the endolymph and 70 to 100 mg/dL in the perilymph.^{15,16} In other words, there are dense protons surrounding K^+ in the endolymph, whereas in the perilymph the protons are relatively sparse. As far as we know, there has been no report on the visualization of endolymphatic hydrops in Ménière's disease by using new non-contrast MRI focusing on the composition of the endolymph and the perilymph of the inner ear.

Therefore, with a special focus on the difference in density of the protons surrounding K^+ in the endolymph and the perilymph, we conducted basic research by MRI of fluids with different concentrations of K^+ and protein. We used an inversion recovery (IR) pulse sequence to evaluate changes in the signal intensity of the fluids. Furthermore, we prepared artificial endolymph and perilymph to explore the optimal inversion time (TI) values, and we found parameters that could be applied to clinical research. Here, we introduce a new method of MRI without contrast agents (new non-contrast MRI). We also examined the relationship between the severity of Ménière's disease and the visualization rate of endolymphatic hydrops, and we report the results.

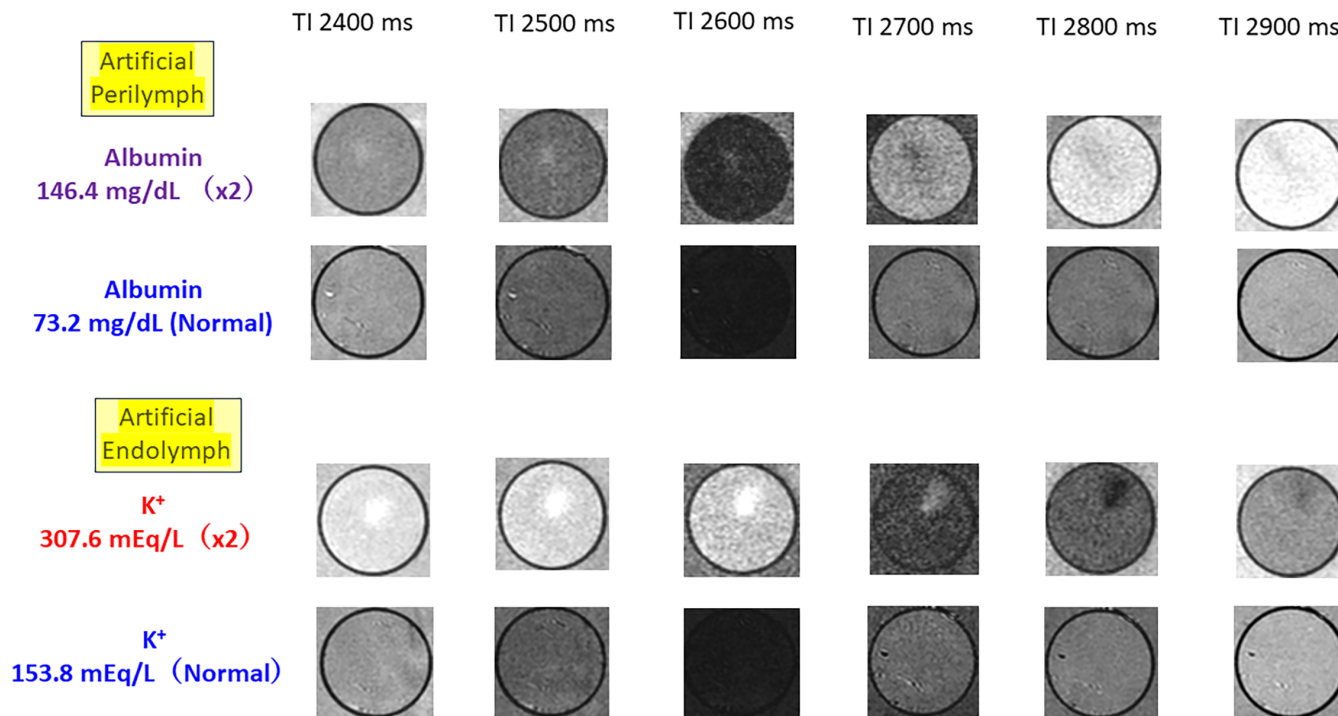


FIGURE 1 Inversion time (TI) multiple time method with increased albumin and K⁺ concentrations in artificial inner ear fluids. There was no difference in TI values at the null point between normal artificial perilymph and endolymph, both being 2600 ms. However, the TI values of artificial perilymph with double the albumin concentration were 2500 to 2600 ms and those of artificial endolymph with double the K⁺ concentration were 2700 to 2800 ms. Subtraction of the positive endolymph image with a high K⁺ concentration from the positive perilymph image with a high protein concentration can yield an important reference value as an imaging parameter in clinical research using the new non-contrast MRI. These phantom experiments on TI changes and contrast comparisons of artificial perilymph and artificial endolymph used multiple TI images. Imaging parameters were: TR = 15,000 ms, TE = 613 ms, TSE factor = 160, and TI = 2000 to 3500 ms at 100-ms intervals. The phantom temperature was approximately 35°C to 36°C.

2 | METHODS AND SUBJECTS

2.1 | Basic experiment (phantom experiment using artificial labyrinthine fluid)

Phantom solutions of artificial endolymph and perilymph containing K⁺ and protein were prepared for the basic research (Figure 1). The artificial endolymph had a high concentration of K⁺ (153.8 mEq/L) and a low concentration of protein (3.84 mg/dL), whereas the artificial perilymph had a low concentration of K⁺ (9.6 mEq/L) and a high concentration of protein (73.2 mg/dL). These concentrations were approximated to the reported respective normal K⁺ and protein concentrations in the endolymph and the perilymph.^{14–16}

The artificial endolymph was prepared by adding KCL solution (20 mL ampoule; 15 w/v%, 2 mol; 40 mEq potassium: Maruishi Pharmaceutical Co. Ltd., Osaka, Japan, generic name: K.C.L.) and albumin solution (human serum albumin 5%, 12.5 g/250 mL, CSL Behring Co. Ltd., generic name: Albuminer) to pure water. The artificial perilymph was prepared by adding the KCL solution and the albumin solution to 0.9% NaCl solution (physiological saline). These solutions of artificial endolymph and perilymph were used as “normal” reference solutions. To examine changes in the TI values due to increases in the K⁺ and albumin concentrations, artificial endolymph with a K⁺

concentration of 307.6 mEq/L (double concentration) and artificial perilymph with an albumin concentration of 146.4 mg/dL (double concentration) were also prepared.

A 3.0-T Ingenia CX with 32-channel head coils (Philips) was used for the experiment in Figure 1. The parameters used for IR were: repetition time (TR) = 15,000 ms; echo time (TE) = 613 ms; turbo spin echo (TSE) factor = 160; and TI = 2000 to 3500 ms at 100-ms intervals (Table 1A). The phantom temperature was approximately 35 to 36°C.

2.2 | Clinical research

In the second stage—the clinical research—both our new non-contrast MRI with the appropriate parameters obtained in the basic research and contrast MRI were performed on the same day. Imaging diagnosis was made by three neuroradiologists who had no conflict of interest with this research. The results were analyzed, and all three doctors made the same diagnosis in the case of patients diagnosed as having endolymphatic hydrops in the inner ear.

The subjects were 50 patients (100 ears) who met the diagnostic criteria for Ménière's disease (No. 1–3) of the Japan Society for Equilibrium Research.¹¹ Thirty-eight of the patients (22 women and 16 men; age 22 to 75 years [mean, 53.3 ± 13.8 years]) underwent both new non-

TABLE 1 MRI systems and parameters.

(A) MRI system: Philips Ingenia CX 3.0-T Head 32-ch coil Phantom			
Temp: 35–36°C			
IR 3D (3.0) T2 weighted 3D IR			
TR: 15,000 ms			
TI: 2000–3000 ms			
TE: 613 ms			
TSE factor: 160			
(B) New non-contrast MRI system: Philips Ingenia CX 3.0-T Head 32-ch coil for Ménière's disease			
PPI (3.0 T) T2-weighted 3D-IR		PEI (3.0 T) T2-weighted 3D-IR	
TR: 15,000 ms		TR: 15,000 ms	
TI: 3050 ms		TI: 2800 ms	
TE: 480 ms		TE: 480 ms	
TSE factor: 109		TSE factor: 109	
(C) Contrast MRI system: Philips Ingenia CX 3.0-T Head 32-ch coil for Ménière's disease			
PPI (3.0 T) T2-weighted 3D-IR		PEI (3.0 T) T2-weighted 3D-IR	
TR: 12,000 ms		TR: 12,000 ms	
TI: 2250 ms		TI: 2050 ms	
TE: 527 ms		TE: 527 ms	
TSE factor: 147		TSE factor: 147	
(D) New non-contrast MRI setup values for Meniere's disease			
Geometry	Non-contrast (Philips)	Contrast (Philips)	Contrast (Siemens)
FOV (mm)	160	200	196
RFOV (%)	100	90	84.4
Matrix scan	240	352	384
Reconstruction	320	640	?
ACQ Voxel MPS (mm)	0.67/0.67/2.0	0.57/0.57/2.0	0.5/0.5/2.0
REC Voxel MPS (mm)	0.5/0.5/1.0	0.31/0.31/1.0	0.5/0.5/1.0
Scan percentage (%)	100	100	100
Sence	2	2	2
Stacks	1	1	1
Slices	55	80	104
Acq slice thickness (mm)	2	2	2
Rec slice thickness (mm)	1	1	1

contrast MRI and contrast MRI. The severity classification of Ménière's disease in these 38 patients was Stage 1 in seven, Stage 2 in seven, Stage 3 in 10, Stage 4 in seven, and Stage 5 in seven. The mean disease duration was 5.3 ± 4.8 years. The remaining 12 patients (24 ears) (all women, age 48 to 74 years [mean, 59.8 ± 7.2 years]), who were under treatment for bronchial asthma and were allergic to contrast agents, underwent only new non-contrast MRI. All of them were in Stage 3. Their mean disease duration was 6.2 ± 3.8 years.

TABLE 2 Ménière's disease severity classification by symptoms.

A:	Balance disorder and daily life impairment
points	
0	Normal
points	
1	Daily activities are sometimes limited (reversible balance disorder)
point	
2	Daily activities are often limited (irreversible mild balance disorder)
points	
3	Daily activities are always limited (irreversible severe balance disorder)
points	
4	Constant limitation of daily activities, difficulty standing and walking in the dark (irreversible bilateral severe balance disorder)
points	
Note	Irreversible bilateral severe balance disorder means that bilateral semicircular canal paralysis is observed in the balance function test
B:	Hearing impairment
points	
0	Normal
points	
1	Reversible (hearing loss limited to low frequencies)
point	
2	Irreversible (irreversible high-frequency hearing loss)
points	
3	Moderate progression (moderate or more irreversible hearing loss)
points	
4	Bilateral severe progression (irreversible bilateral severe hearing loss)
points	
Note	Note: Irreversible bilateral severe hearing loss means that the average hearing level is 70 dB or more on both sides and does not improve to less than 70 dB in pure tone audiometry
C:	Degree of disease progression
points	
0	Only lifestyle guidance is given and follow-up observation is performed.
points	
1	Conservative treatment is required for reversible lesions.
point	
2	Irreversible lesions progress even with conservative treatment.
points	
3	Lesions progress severely and resist conservative treatment, and invasive treatment is considered.
points	
4	Irreversible lesions progress severely and leave sequelae.
points	
Ménière's disease comprehensive severity classification	
Stage 1: Subnormal period A: 0 points; B: 0 points; C: 0 points	
Stage 2: Reversible period A: 0–1 points; B: 0–1 points; C: 1 point	
Stage 3: Irreversible period A: 1–2 points; B: 1–2 points; C: 2 points	
Stage 4: Progressive period A: 2–3 points; B: 2–3 points; C: 3 points	
Stage 5: Sequelae period A: 4 points; B: 4 points; C: 4 points	

Note: Symptoms of Ménière's Disease are classified into: A: Balance disorder and daily life impairment; B: Hearing impairment; and C: Degree of disease progression. The comprehensive severity classification consists of five stages based on the total of the points for A, B, and C.¹⁸

These cases of Ménière's disease were classified on the basis of severity¹⁷ (Table 2). This was done by summing up the severity of symptoms for (A) Balance disorder and daily life impairment;

(B) Hearing impairment; and (C) Degree of disease progression, and classifying them into five stages. Hearing impairment included reversible low-frequency hearing loss, irreversible high-frequency hearing loss, moderate hearing loss, and severe bilateral hearing loss. All subjects were limited to those who were able to have MRI exam within 1 month after attacks of Ménière's disease.

Verbal and written informed consent was obtained from all patients before the series of examinations. Following new non-contrast MRI (see imaging parameters in Table 1B and setup values in Table 1D), contrast MRI was performed 4 h after the administration of GBCA ($C_{18}H_{31}GdN_4O_9$, Gadovist; Bayer Healthcare Pharmaceuticals, Co. Ltd., Osaka, Japan, generic name: Gadobutrol), at 0.1 mmol/kg. A 3.0-T Ingenia CX with 32-channel head coils (Philips) was used. The imaging parameters used for the contrast MRI are shown in Table 1C. Statistical analysis of the data was performed on a Windows 10 PC by using add-on software (Statcel Ver. 5, Microsoft Excel) dedicated to statistical analysis.

3 | RESULTS

3.1 | Results of basic research

An important feature of this phantom experiment is that images of the perilymph with normal and double albumin concentrations were compared and those of endolymph with normal and double K^+ concentrations were also compared. There was no difference in T1 values at the null point between normal artificial perilymph and endolymph, both being 2600 ms. However, the T1 values of artificial perilymph with double the albumin concentration were 2500 to 2600 ms and those of artificial endolymph with double the K^+ concentration were 2700 to 2800 ms.

In other words, the T1 value at the null point was the same between the artificial endolymph with normal K^+ concentration and the artificial perilymph with normal albumin concentration. When the K^+ concentration was increased in the artificial endolymph, the T1 value at the null point was prolonged; when the albumin

concentration was increased in the perilymph, the T1 value at the null point was shortened. The IR longitudinal magnetization recovery process (T1 relaxation) can be assumed from the changes in the T1 values at the null point (Figure 2). The T1 values were shortened with increasing albumin concentration; in contrast, the T1 values were prolonged with increasing K^+ concentration. This suggested the possibility of separating the images of perilymph and endolymph.

These results suggest that, if increased K^+ in the endolymph and increased protein in the perilymph are involved in the pathogenesis of Ménière's disease, then subtracting the PEI with high K^+ and low protein concentrations from the PPI with low K^+ and high protein concentrations could provide new parameters for new non-contrast MRI.

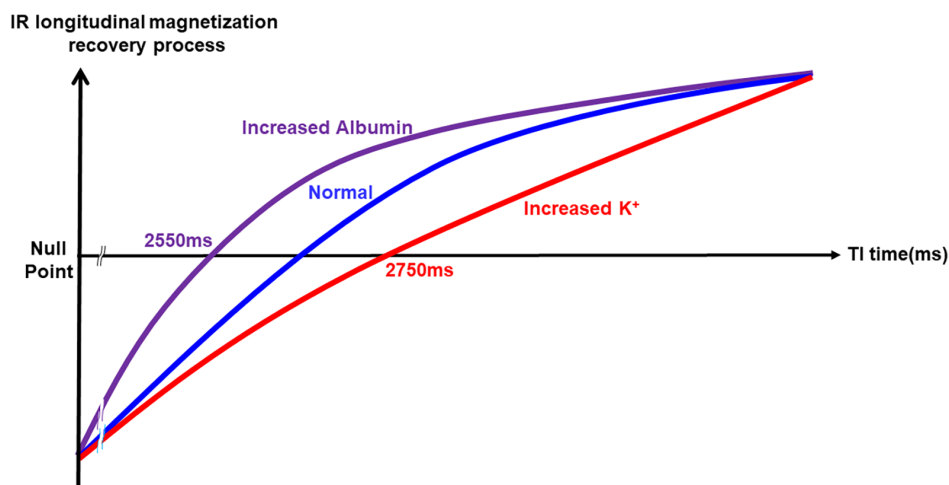
3.2 | Results of clinical research

From the results of the basic research over many years, we pursued the null point of the PPI with a high albumin concentration and that of the PEI with a high K^+ concentration in our clinical research. The null point of the PPI was eventually found to be 3050 ms and that of the PEI was found to be 2800 ms (Table 1B).

We created schematic diagrams of the contrast and new non-contrast-enhanced MRI imaging methods used for endolymphatic hydrops (Figure 3). The upper row shows the contrast MRI imaging method, in which images are obtained by subtracting the PEI from the PPI 4 h after intravenous administration of the GBCA (HYDROPS).⁸⁻¹⁰ The bottom row shows the new non-contrast MRI imaging method, in which images are obtained by subtracting the PEI from the PPI. The T1 values of the PPI and the PEI differed markedly between contrast MRI and the new non-contrast MRI. The other imaging parameters of MRI set up values (Geometry) were also substantially different (Table 1D).

Here, we present clinical cases of patients with Ménière's disease who underwent the contrast or new non-contrast MRI, or both, using above mentioned parameters. Figure 4 shows an image of GBCA contrast-enhanced MRI and an image of the new non-contrast MRI

FIGURE 2 Inversion recovery (IR) longitudinal magnetization recovery process of artificial inner ear fluid (T1 relaxation). A graph of the IR longitudinal magnetization recovery process (T1 relaxation) assumed from the null point is shown. The blue curve represents the artificial inner ear fluid with almost normal concentrations of K^+ and albumin, the red curve represents the artificial endolymph with increased K^+ concentration, and the purple curve represents the artificial perilymph with increased albumin.



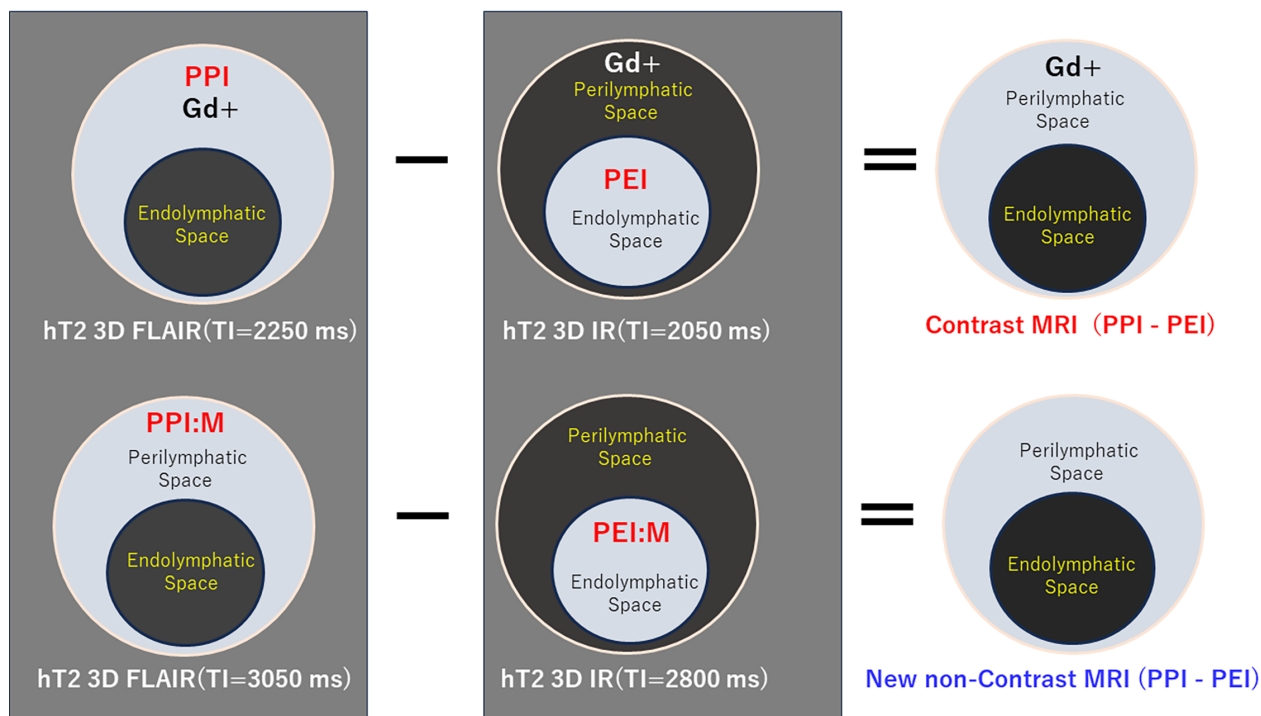


FIGURE 3 Schematic diagram of methods of imaging endolymphatic hydrops by contrast and new non-contrast-enhanced MRI. The upper row shows the contrast MRI imaging method, in which images are obtained by subtracting the positive endolymph image (PEI) from the positive perilymph image (PPI) 4 h after the intravenous administration of a gadolinium-based contrast agent. The lower row shows the new non-contrast MRI imaging method. The inversion time (TI) values used in the newly developed new non-contrast MRI, with reference to basic experiments, differed markedly from those used in the contrast MRI. Gd+, gadolinium.

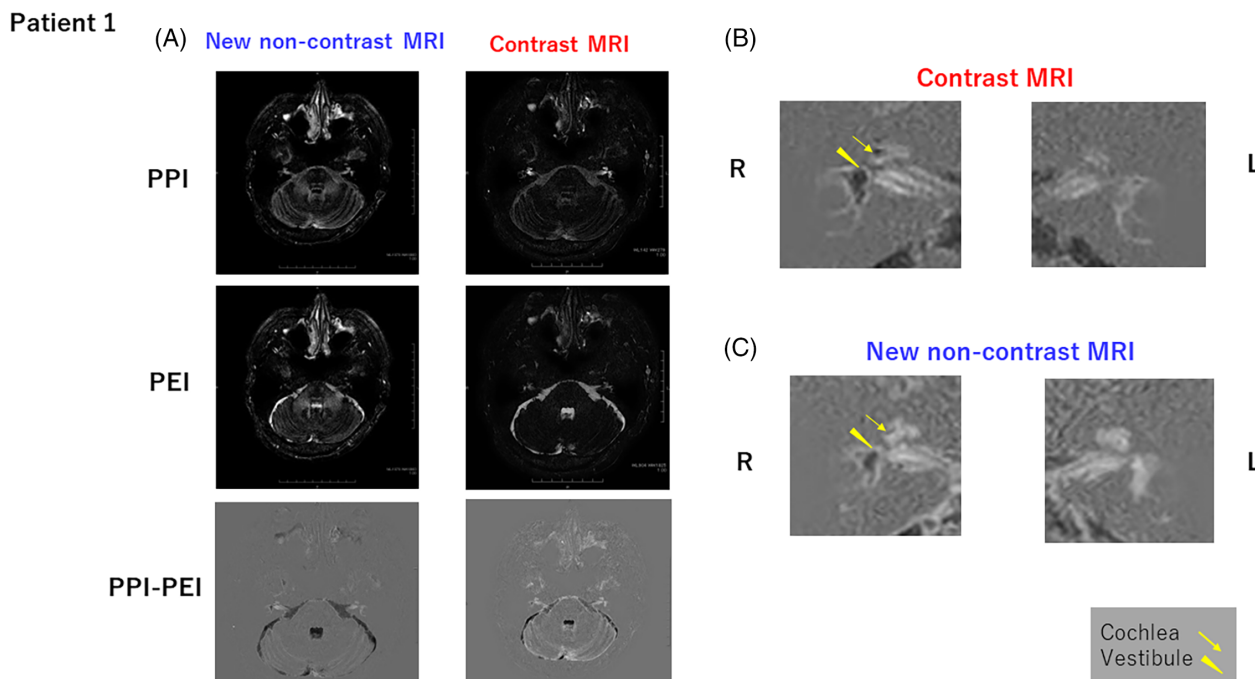


FIGURE 4 Contrast and new non-contrast MRI of Patient 1 (PPI, PEI, and PPI - PEI). (A) Positive perilymph image (PPI), positive endolymph image (PEI), and PPI - PEI by contrast MRI and the new non-contrast MRI. (B) Magnified images of the inner ears by contrast MRI. (C) Magnified images of the inner ears by new non-contrast MRI. Patient 1 was a 49-year-old man with Stage 3 right-sided Ménière's disease. Lesions with decreased signal intensity are apparent in the new non-contrast MRI; they are consistent with images considered to represent endolymphatic hydrops in the right vestibule and cochlea.

Patient 2

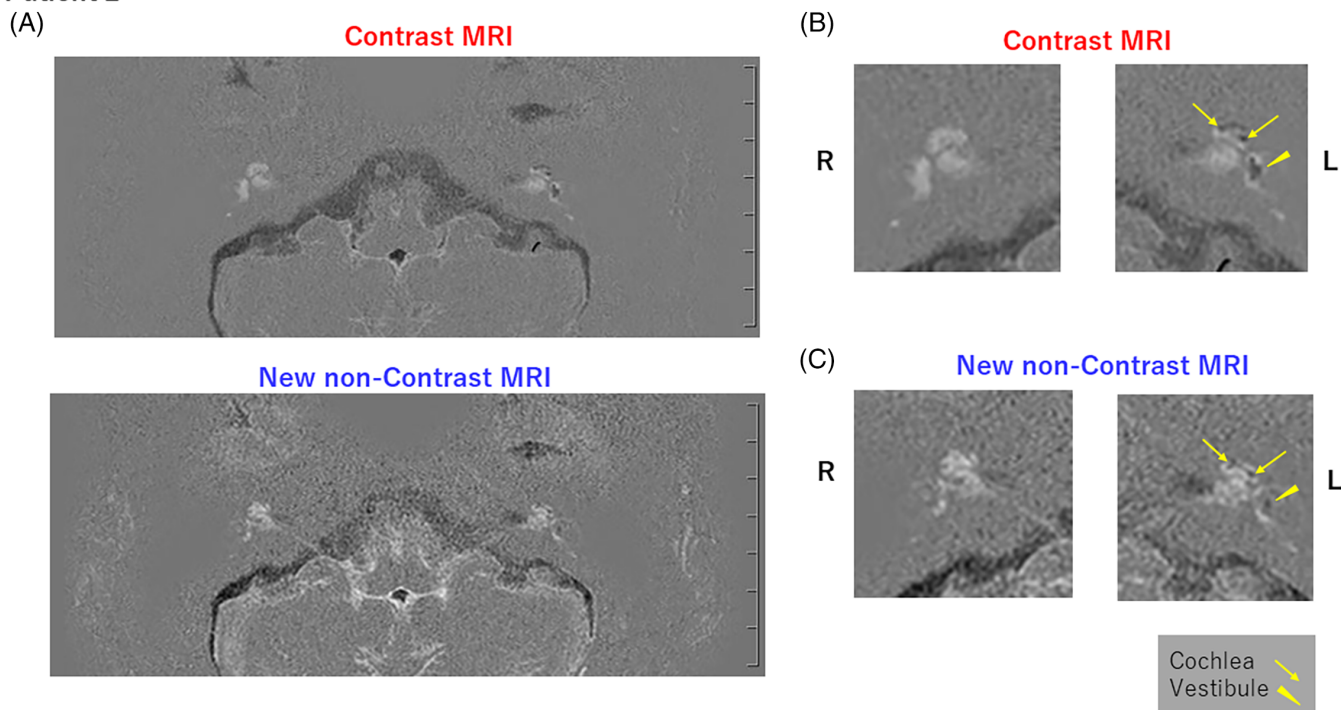


FIGURE 5 Images comparing contrast and new non-contrast MRI of Patient 2. Patient 2 was a 25-year-old man with Stage 4 left-sided Ménière's disease. (A) Images of the inner ear at the cerebellopontine angle: The upper row is contrast MRI and the lower row is new non-contrast MRI. (B) Magnified images of the inner ears by contrast MRI. (C) Magnified images of the inner ears by new non-contrast MRI. Lesions with decreased signal intensity are apparent in the new non-contrast MRI; they are consistent with images considered to represent endolymphatic hydrops in the left vestibule and cochlea.

created in a patient with Ménière's disease by subtracting the PEI from the PPI using the parameters in Table 1B,C. Patient 1 was a 49-year-old man with Stage 3, right-sided Ménière's disease who had right-sided hearing loss and had the disease for 2 years and 10 months. Lesions with decreased signal intensity are apparent in the new non-contrast MRI; they are consistent with images considered to be endolymphatic hydrops in the right vestibule and cochlea.

Figure 5 shows contrast and new non-contrast MRI of Patient 2. Patient 2 was a 25-year-old man with Stage 4 left-sided Ménière's disease who had left-sided severe hearing loss and had the disease for 3 years and 7 months. Lesions with decreased signal intensity are apparent in the new non-contrast MRI; they are consistent with images considered to be endolymphatic hydrops in the left vestibule and cochlea.

Figure 6 shows contrast and new non-contrast MRI of Patient 3, who was a 34-year-old woman with Stage 3 right-sided Ménière's disease. Lesions with decreased signal intensity are apparent in the new non-contrast MRI; they are consistent with images considered to be endolymphatic hydrops in the left vestibule and cochlea.

Figure 7 shows new non-contrast MRI of Patient 4. Patient 4 was a 61-year-old woman with Stage 3 right-sided Ménière's disease and asthma, with allergy to contrast agents. Patient 4 had moderate left low- to middle-tone hearing loss and had the disease for 8 years and 5 months. Lesions with decreased signal intensity consistent with symptoms are evident on the new non-contrast MRI, consistent

with imaging and symptoms of possible endolymphatic hydrops of the right vestibule and cochlea.

Figure 8 shows new non-contrast MRI of Patients 5 and 6. Patient 5 was a 47-year-old woman with Stage 3 right-sided Ménière's disease who had moderate right-sided low- to high-tone hearing loss and had the disease for 3 years and 7 months. Patient 6 was a 51-year-old woman with Stage 3 left-sided Ménière's disease who had moderate left low- to middle-tone hearing loss and had the disease for 4 years and 2 months. Both patients underwent only new non-contrast MRI, because they had asthma and were allergic to contrast media. Lesions in Patients 5 and 6 with decreased signal intensity are apparent in the new non-contrast MRI; they are consistent with images considered to represent endolymphatic hydrops in the vestibule and cochlea.

Figure 9 shows new non-contrast MRI of Patient 7. Patient 7 was a 52-year-old woman with Stage 3 right-sided Ménière's disease who had moderate left-sided low- to high-tone hearing loss and had the disease for 4 years and 9 months. Patient 7 underwent only new non-contrast MRI, because she had asthma and was allergic to contrast media. Lesions with decreased signal intensity are apparent in the new non-contrast MRI; they are consistent with images considered to represent endolymphatic hydrops in the vestibule and cochlea.

Table 3 shows the visualization rates of endolymphatic hydrops in the cochlea and the vestibule of 38 patients (76 ears) who underwent both novel non-contrast MRI and contrast MRI. The visualization rate of endolymphatic hydrops in the cochlea was very low on novel non-

Patient 3

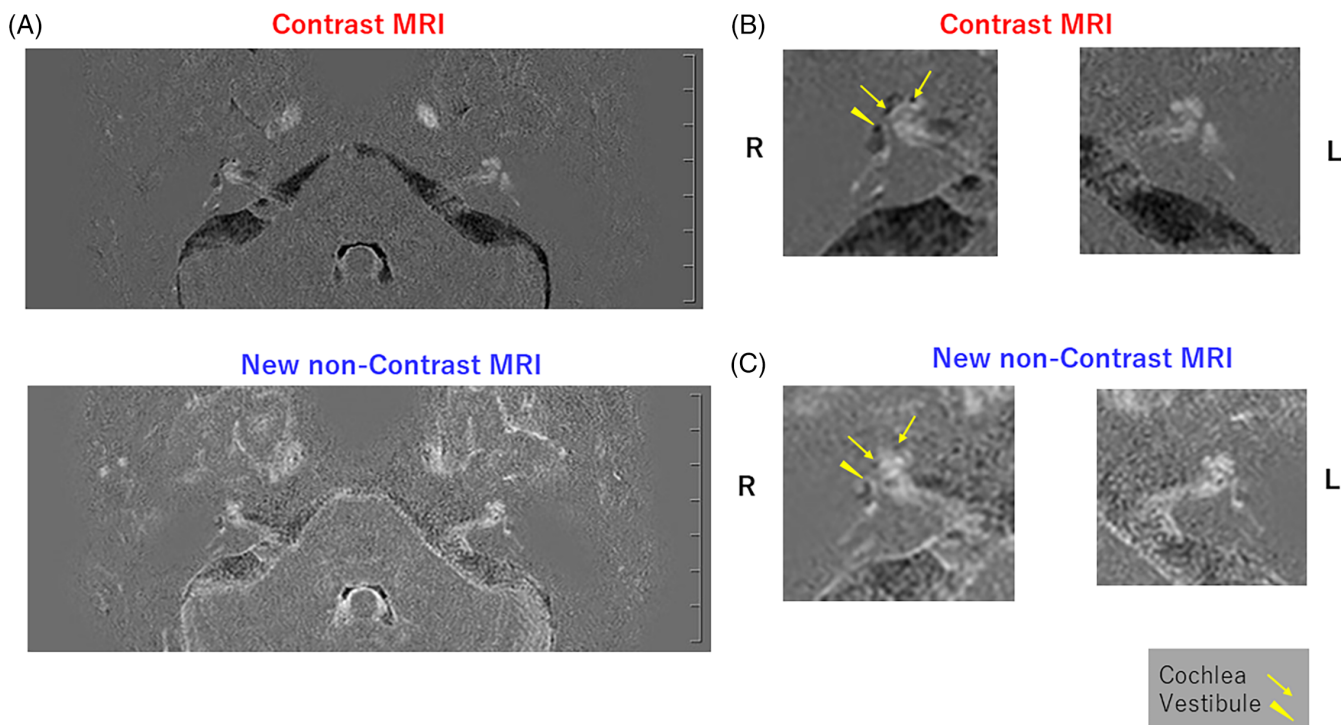


FIGURE 6 Images comparing contrast and new non-contrast MRI of Patient 3. Patient 3 was a 34-year-old woman with Stage 3 right-sided Ménière's disease. (A) Images of the inner ear at the cerebellopontine angle: The upper row is contrast MRI and the lower row is new non-contrast MRI. (B) Magnified images of the inner ears by contrast MRI. (C) Magnified images of the inner ears by new non-contrast MRI. Lesions with decreased signal intensity are apparent in the new non-contrast MRI; they are consistent with images considered to represent endolymphatic hydrops in the left vestibule and cochlea.

Patient 4

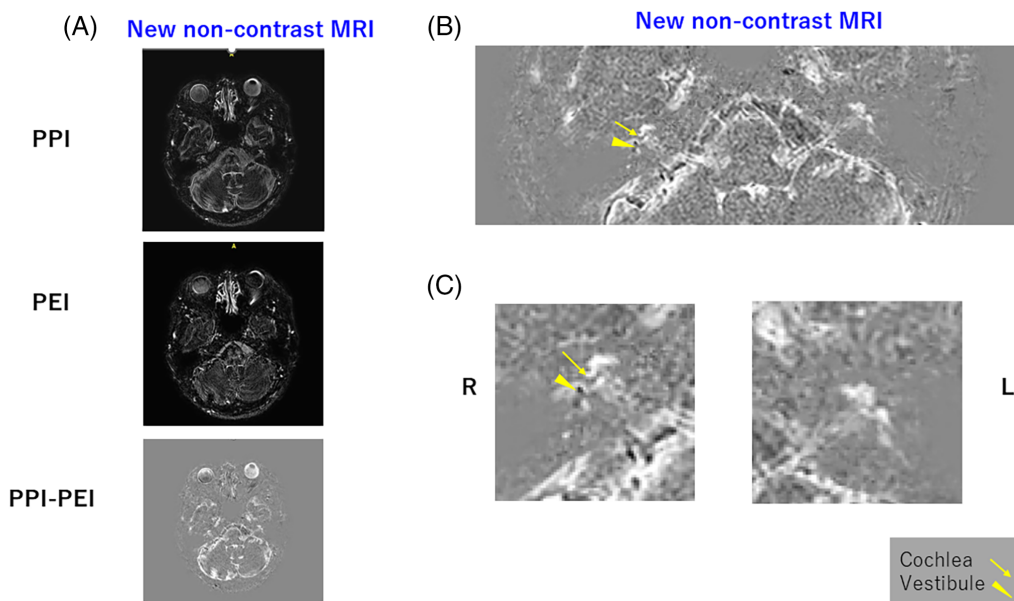
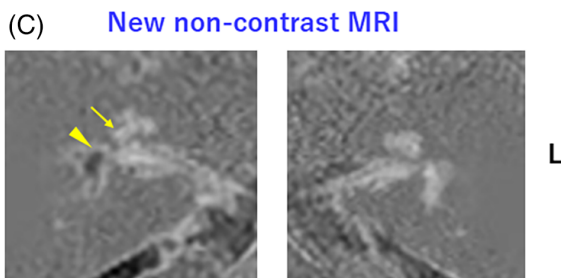
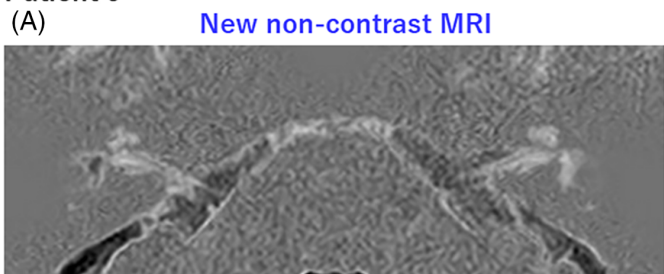


FIGURE 7 New non-contrast MRI of Patient 4. Patient 4 was a 61-year-old woman with Stage 3 right-sided Ménière's disease. (A) Positive endolymph image (PPI), positive endolymph image (PEI), and PPI - PEI. (B) Inner ear at the cerebellopontine angle. (C) Magnified images of the inner ear. On new non-contrast MRI, lesions are evident with decreased signal intensity and consistent with imaging and symptoms of possible endolymphatic hydrops of the right vestibule and cochlea.

Patient 5



Patient 6

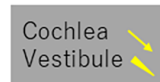
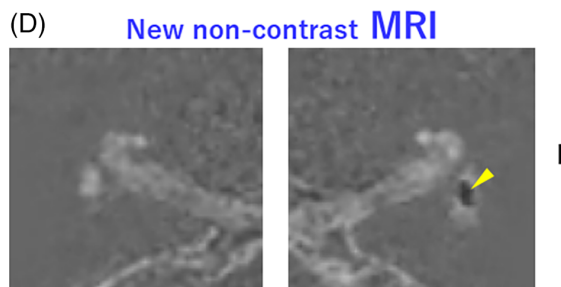
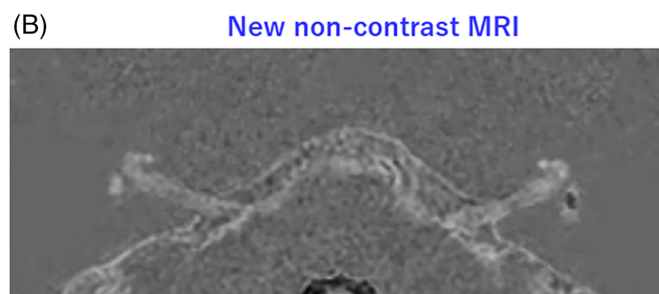


FIGURE 8 New non-contrast MRI of Patients 5 and 6. Patient 5 was a 47-year-old woman with Stage 3 right-sided Ménière's disease. Patient 6 was a 51-year-old woman with Stage 3 left-sided Ménière's disease. (A) Image of the inner ear at the cerebellopontine angle of Patient 5. (B) Image of Patient 6. (C) Magnified images of the inner ears of Patient 5, and (D) magnified images of the inner ears of Patient 6. Lesions in Patients 5 and 6 with decreased signal intensity are apparent in the new non-contrast MRI; they are consistent with the images considered to represent endolymphatic hydrops in the vestibule and cochlea.

Patient 7

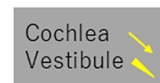
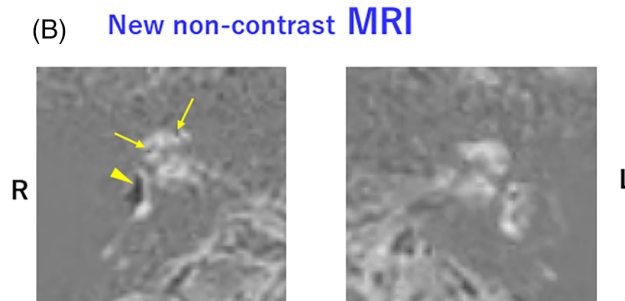
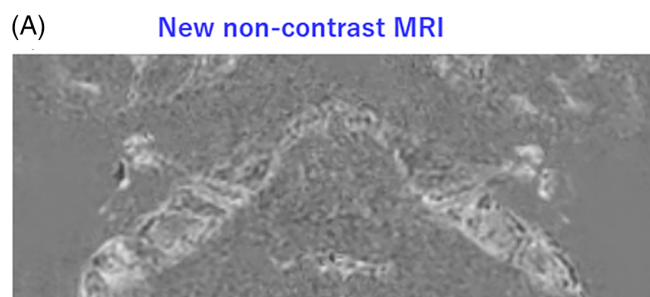


FIGURE 9 New non-contrast MRI of Patient 7. Patient 7 was a 52-year-old woman with Stage 3 right-sided Ménière's disease. (A) Image of the inner ear at the cerebellopontine angle; (B) magnified images of the inner ears. Lesions with decreased signal intensity in Patient 7 are apparent in the new non-contrast MRI; they are consistent with images considered to represent endolymphatic hydrops in the vestibule and cochlea.

contrast MRI (28.9%) compared with that on contrast MRI (71.1%). The visualization rate in the vestibule was 65.8% on novel non-contrast MRI and 84.2% on contrast MRI. However, there was no significant difference in the visualization rate of endolymphatic hydrops between contrast MRI and the novel non-contrast MRI, or between

the cochlea and the vestibule (2×2 contingency table: Chi-square test for independence).

Next, we plotted the visualization rates of endolymphatic hydrops with contrast MRI and the new non-contrast MRI by stage of disease severity (Figure 10). There was no significant difference in the

visualization rates of endolymphatic hydrops between Stages 1 and 2 (n.s. by the chi-square test) or among Stages 3 to 5 (n.s. by the chi-square test). However, the visualization rate for Stages 3 to 5 as a group was significantly greater than that for Stages 1 and 2 as a group (chi-square test for independence, $p < .01$). Also, the visualization rate of endolymphatic hydrops in patients at all stages was significantly greater with contrast MRI than with the new non-contrast MRI ($m \times n$ contingency table: chi-square test for independence, $p < .01$).

4 | DISCUSSION

Endolymphatic hydrops in patients with Ménière's disease has been demonstrated by non-contrast MRI using T2 preparations (T2Preps) technique.¹⁸ However, problems of artifacts and noise with the

TABLE 3 Visualization rates of endolymphatic hydrops in the cochlea and the vestibule of 38 patients with Ménière's disease.

	Cochlea	Vestibule
Contrast MR	75.5%	81.8%
New non-contrast MRI	27.3%	63.6%

Note: The visualization rate of endolymphatic hydrops in the cochlea by novel non-contrast MRI was very low, and that in the vestibule by novel non-contrast MRI was also lower than that by contrast MRI. However, there was no significant difference between the visualization rates with novel non-contrast MRI and those with contrast MRI or between the rates for the cochlea and those for the vestibule (2×2 contingency table: Chi-square test for independence, no significant). 2×2 contingency table: Chi-square test for independence N.S.

technique have been pointed out.^{19,20} As a preliminaries test to our study, on the basis of that report,¹⁸ we verified the technique in six normal controls and five patients with Ménière's disease. That results showed no significant difference in the vestibular images between normal controls and patients with Ménière's disease, and no clear difference between the affected and healthy sides. Therefore, an alternative non-contrast-agent method was required.

The pathogenesis of Ménière's disease is still mostly unknown. However, we have been studying the autonomic nervous system in detail in these patients for over 10 years. We have found that overexcitation of sympathetic nerves on the affected side occurs immediately before an attack of Ménière's disease, and we recently reported this finding.²¹ Overexcitation of the sympathetic nervous system, which is closely related to stress, causes contraction of arterioles distributed in the inner ear. This generates shear stress in the blood vessels, leading to increased K^+ in the blood vessels and increased vascular permeability.²² Increased vascular permeability causes extravascular leakage of albumin.²³ Increased K^+ in the perilymph leads to increased K^+ in the endolymph by the potassium ion cycle,²⁴ and the resulting neurotoxicity can be assumed to cause hearing impairment, nystagmus, and vertigo.^{21,25,26} Furthermore, increased K^+ leads to a decrease in hydration kinetics (negative hydration),^{27,28} resulting in the prolongation of T1 values; in contrast, increased albumin leads to an increase in hydration kinetics (positive hydration),²⁹ resulting in the shortening of T1 values. Therefore, this difference in T1 values enables us to separate the endolymph and perilymph.

Image analysis focusing on K^+ in the endolymph could be important for determining the cause of the disease. By using the results of

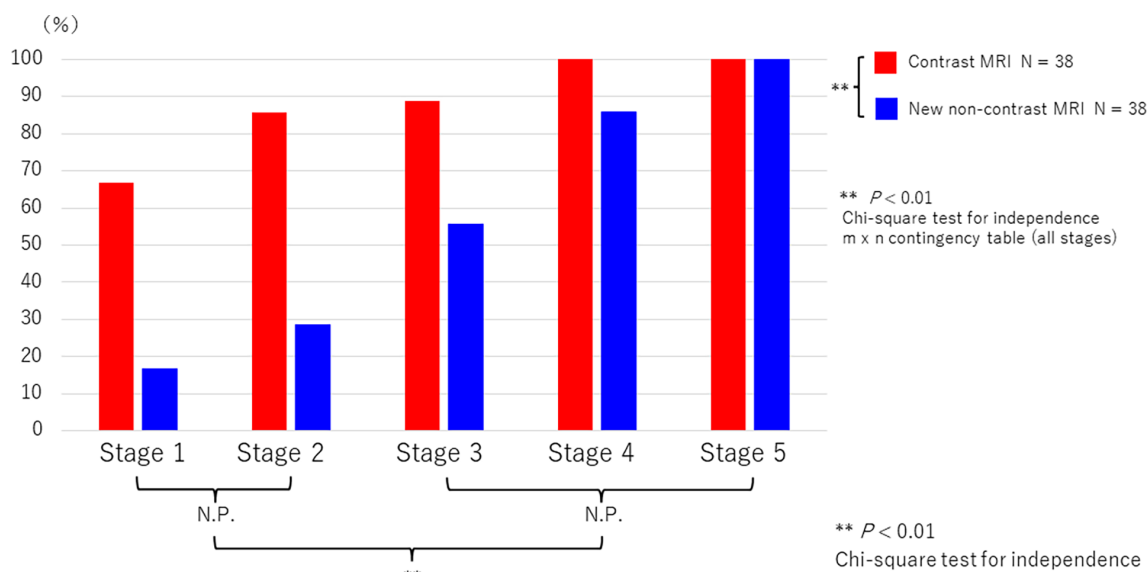


FIGURE 10 Severity stages and visualization rates of endolymphatic hydrops. Analysis of the relationship between Ménière's disease severity stage and visualization rate of endolymphatic hydrops by contrast MRI and the new non-contrast MRI. The visualization rate for Stages 3 to 5 as a group was significantly greater than that for Stages 1 and 2 as a group (chi-square test for independence, $p < .01$). Also, the visualization rate of endolymphatic hydrops in patients at all stages was significantly greater with contrast MRI than with the new non-contrast MRI ($m \times n$ contingency table: Chi-square test for independence, $p < .01$).

our basic research, we explored in detail the parameters that could be used to separate the endolymph from the perilymph on MRI. In other words, we tried to reduce image artifacts and noise to increase the resolution as much as possible. We finally found parameters by which the new non-contrast MRI differed markedly from contrast MRI (Table 1D). This enabled us to create images that could separate the endolymph from the perilymph (Table 1C; Figures 2 and 3).

The values for the null point for PPI and PEI—the point at which the artificial endolymph and perilymph could be separated—were lower than those in the actual clinical setting (PPI: 3050 ms; PEI: 2800 ms) (see Figure 2 and Table 1B). This was likely because, unlike in the artificial setting, (i) the core body temperature is around 37°C; (ii) the inner ear has a hard bony capsule and surrounding mastoid air cells; (iii) there is a flow in the inner ear lymph^{30–32}; and (iv) the endolymph and perilymph contain electrolytes other than K⁺ at different concentrations.^{14,15} In our clinical research, comparison of the visualization rates of endolymphatic hydrops in the cochlea and the vestibule by using the new non-contrast MRI and contrast MRI showed that the visualization rates of endolymphatic hydrops in the cochlea tended to be lower with the former than with the latter (see Table 3). This may have been due to the presence of the hard bony capsule around the cochlea and the small volume of the endolymph.

In patients with severe Ménière's disease (Stages 3 to 5), visualization rates of endolymphatic hydrops on the affected side increased with increasing stage (see Figure 10). Endolymphatic hydrops was not visualized on the healthy side in these patients. These findings are extremely important for understanding the pathophysiology of Ménière's disease. Our new non-contrast MRI used parameters focusing on changes in the K⁺ concentration of endolymph and changes in the protein concentration of perilymph; therefore, our results may have suggested that there was an increased K⁺ concentration in the endolymph on the affected side and an unchanged K⁺ concentration on the healthy side. Another reason for the non-visualization of endolymphatic hydrops on the healthy side by our method may have been that the volume of endolymphatic hydrops was too small on that side.

This new method of new non-contrast MRI will make it easier, not only to follow up patients with severe Ménière's disease at higher stages immediately after an attack and thereafter, but also to understand changes in the pathophysiology of the inner ear. Further studies are important and necessary. Because the resolution of our new non-contrast MRI is currently relatively low, classification by using the quantitative analysis of endolymphatic hydrops visualized by using contrast-enhanced MRI³³ cannot yet be applied.

Although we used a 3.0-T MRI scanner with 32-channel head coils in our clinical research, within our research group we have confirmed that, with the use of the same parameters, the same MRI scanner model with 20-channel head and neck coils can provide images of a quality comparable to that of images obtained with a 3.0-T MRI scanner with 32-channel head coils. Use of the same parameters as we have used here will enable the use of other manufacturers' models to visualize endolymphatic hydrops. We consider this to be a future task.

5 | CONCLUSIONS

We devised a new non-contrast MRI method with parameters focusing on protein and protons closely surrounding K⁺ to visualize endolymphatic hydrops in Ménière's disease. The method enabled us to visualize endolymphatic hydrops at high rates in patients at Stage 3 or higher, consistent with the symptomatic, affected side. Therefore, this new non-contrast MRI method will be useful and helpful in patients with clinically problematic Stage 3 or higher Ménière's disease who have restrictions on, or contraindications for, the use of contrast agents. We expect that improvement and enhancement in MRI signal processing will provide greater diagnostic power. Our new non-contrast MRI method has the potential to help us understand the pathophysiological changes that occur immediately after a Ménière's attack and thereafter.

ACKNOWLEDGMENTS

We sincerely thank Dr. Kazuya Nakamoto, Chief Director of the Ochanomizu Clinic, for his unwavering support during this study. We also thank Dr. Seishi Sawano, Clinical Director of AIC Yaesu Clinic, and Mr. Tatsuya Otsuka, Secretary General of the Yaesu Clinic, for their support with ethics and equipment.

AUTHOR CONTRIBUTIONS

HT, RA, Y Kanai, MY and MI initiated and designed the study and RA, Y Kanai and MI collected data. RA, Y Kanai, and MI conducted the data analysis, and MI wrote the main manuscript text. HT, RA, Y Kanai, Y Kato, YI, FM, MY, GI, and AI reviewed the manuscript.

CONFLICT OF INTEREST STATEMENT

The authors declare no conflicts of interest.

ORCID

Masanori Ishii  <https://orcid.org/0000-0002-3452-8677>

Gail Ishiyama  <https://orcid.org/0000-0003-4382-8089>

REFERENCES

- Baloh RW. Prosper Ménière and his disease. *Arch Neurol*. 2001;58(7):1151–1156. doi:10.1001/archneur.58.7.1151
- Hallpike CS, Cairns H. Observations on the pathology of Meniere's syndrome. *J Laryngol Otol*. 1938;53:625–655.
- Yamakawa K. Über die pathologische Veränderung bei einem Meniere-Kranken [on the pathological changes in a patient with Meniere's disease]. *Z Hals-, Nasen- u Ohrenheilkd*. 1938;32:697. (German).
- Committee on Hearing and Equilibrium. Guidelines for the diagnosis and evaluation of therapy in Meniere's disease. *Otolaryngol Head Neck Surg*. 1995;113(1):181–185. doi:10.1016/S0194-5998(95)70102-8
- Goebel JA. 2015 Equilibrium Committee Amendment to the 1995 AAO-HNS guidelines for the definition of Ménière's disease. *Otolaryngol Head Neck Surg*. 2016;154(2):403–404. doi:10.1177/0194599816628524
- Lopez-Escamez JA, Carey J, Chung WH, et al. Diagnostic criteria for Ménière's disease. *J Vestibul Res*. 2015;25:1–71. doi:10.3233/VES-150549

7. Nakashima T, Naganawa S, Sugiura M, et al. Visualization of endolymphatic hydrops in patients with Ménière's disease. *Laryngoscope*. 2007;17:415-420. doi:[10.1097/MLG.0b013e31802c300c](https://doi.org/10.1097/MLG.0b013e31802c300c)
8. Naganawa S, Yamazaki M, Kawai H, et al. Imaging of Meniere's disease after intravenous administration of single-dose gadodiamide: utility of subtraction images with different inversion times. *Magn Reson Med Sci*. 2012;11:213-219. doi:[10.2463/mrms.11.213](https://doi.org/10.2463/mrms.11.213)
9. Naganawa S, Kawai H, Taoka T, Sone M. Improved HYDROPS: imaging of endolymphatic hydrops after intravenous administration of gadolinium. *Magn Reson Med Sci*. 2017;16:357-361. doi:[10.2463/mrms.tn.2016-0126](https://doi.org/10.2463/mrms.tn.2016-0126)
10. Naganawa S, Nakashima T. Visualization of endolymphatic hydrops with MR imaging in patients with Ménière's disease and related pathologies: current status of its methods and clinical significance. *J Jpn Radiol Soc*. 2014;74:191-204. doi:[10.1007/s11604-014-0290-1](https://doi.org/10.1007/s11604-014-0290-1)
11. Iwasaki S, Shojaku H, Moutushi T, et al. Committee for Clinical Practice Guidelines of Japan Society for Equilibrium Research. Research diagnostic and therapeutic strategies for Ménière's disease of the Japan Society for Equilibrium Research. *Auris Nasus Larynx*. 2021;48:15-22. doi:[10.1016/j.anl.2020.10.009](https://doi.org/10.1016/j.anl.2020.10.009)
12. Ohtaki H, Radnai T. Structure and dynamics of hydrated ions. *Chem Rev*. 1993;93:1157-1204. doi:[10.1021/cr00019a014](https://doi.org/10.1021/cr00019a014)
13. Mochizuki K, Sugawara K, Kameda Y, Usuki T, Uemura O. Hydration structure of the potassium ion determined by combined analysis of neutron and X-ray diffraction data. *Advances in Neutron Scattering Research*. Japan Physical Society; 2001:371-373. (Suppl A to *J Phys Soc Jpn*).
14. Konishi T, Hamrick PE, Walsh PJ. Ion transport in Guinea pig cochlea. I. Potassium and sodium transport. *Acta Otolaryngol*. 1978;86(1-2):22-24. doi:[10.3109/00016487809124717](https://doi.org/10.3109/00016487809124717)
15. Rauch S, Kostlin A. Aspects chimiques de l'endolymph et de la périlymphe [chemical aspects of endolymph and perilymph]. *Pract Otorhinolaryngol (Basel)*. 1958;20:287-291. (French).
16. Salt AK, DeMott PJ. Potassium and sodium fluxes in the endolymph and perilymph of the Guinea pig cochlea. *Hear Res*. 1989;41:35-49. doi:[10.1016/0378-5955\(89\)90014-9](https://doi.org/10.1016/0378-5955(89)90014-9)
17. Ikezono T, Itoh A, Takeda N, et al. Materials for standardization of diagnosis of vertigo. Diagnostic criteria revised. *Equilibrium Res*. 2010;76:233-241.
18. Fukutomi H, Hamitouche L, Yamamoto T, et al. Visualization of the saccule and utricle with non-contrast-enhanced FLAIR sequences. *Eur Radiol*. 2022;32:3532-3540. doi:[10.1007/s00330-021-08403-w](https://doi.org/10.1007/s00330-021-08403-w)
19. Kato Y, Naganawa S, Taoka T, Yoshida T, Sone M. Pitfalls of using T2-contrast enhancement techniques in 3D-FLAIR to detect endolymphatic hydrops. *Magn Reson Med Sci*. 2023;22:335-344. doi:[10.2463/mrms.mp.2022-0017](https://doi.org/10.2463/mrms.mp.2022-0017)
20. Ichinose N, Haraoka K, Mori T, Ozaki M, Taniguchi A. Effect of the surrounding magnetic environment of temporal bone on the fluid signal intensity in human inner ear using a combined T2 preparation pulse and fluid attenuated inversion pulse technique. *Magn Reson Med Sci*. 2023;1-11. doi:[10.2463/mrms.mp.2023-0074](https://doi.org/10.2463/mrms.mp.2023-0074)
21. Ishii M, Ishiyama G, Ishiyama A, Kato Y, Mochizuki F, Ito Y. Relationship between the onset of Ménière's disease and sympathetic hyperactivity. *Front Neurol*. 2022;13:804777. doi:[10.3389/fneur.2022.804777](https://doi.org/10.3389/fneur.2022.804777)
22. Kadry H, Noorani B, Cucullo L. A blood-brain barrier overview on structure, function, impairment, and biomarkers of integrity. *Fluids Barriers CNS*. 2020;17:69. doi:[10.1186/s12987-020-00230-3](https://doi.org/10.1186/s12987-020-00230-3)
23. Kumar P, Shen Q, Pivetti CD, Lee ES, Wu MH, Yuan SY. Molecular mechanisms of endothelial hyperpermeability: implications in inflammation. *Expert Rev Mol Med*. 2009;11:19. doi:[10.1017/S1462399409000112](https://doi.org/10.1017/S1462399409000112)
24. Spicer SS, Schulte BA. Evidence for a medial K⁺ recycling pathway from inner hair cells. *Hear Res*. 1998;118(1-2):1-12. doi:[10.1016/S0378-5955\(98\)00006-9](https://doi.org/10.1016/S0378-5955(98)00006-9)
25. Kakigi A, Salt AN, Takeda T. Effect of artificial endolymph injection into the cochlear duct on perilymph potassium. *ORL J Otorhinolaryngol Relat Spec*. 2010;71(Suppl 1):16-18. doi:[10.1159/000265118](https://doi.org/10.1159/000265118)
26. Brown DJ, Chihara Y, Wang Y. Changes in utricular function during artificial endolymph injections in Guinea pigs. *Hear Res*. 2013;304:70-76. doi:[10.1016/j.heares.2013.05.011](https://doi.org/10.1016/j.heares.2013.05.011)
27. Conte P. Effects of ions on water structure: a low-field ¹H T₁ NMR relaxometry approach. *Magn Reson Chem*. 2015;53:711-718. doi:[10.1002/mrc.4174](https://doi.org/10.1002/mrc.4174)
28. Geiger A. Molecular dynamics simulation study of the negative hydration effect in aqueous electrolyte solutions. *Ber Bunenges Phys Chem*. 1981;85:52-63. doi:[10.1002/bbpc.19810850112](https://doi.org/10.1002/bbpc.19810850112)
29. Bydder GM, Young IR. MR imaging: clinical use of the inversion recovery sequence. *J Comput Assist Tomogr*. 1985;9:659-675.
30. Salt AN, DeMott J. Longitudinal endolymph flow associated with acute volume increase in the Guinea pig cochlea. *Hear Res*. 1997;107:29-40. doi:[10.1016/S0378-5955\(97\)00018-X](https://doi.org/10.1016/S0378-5955(97)00018-X)
31. Ciunan RR. Stria vascularis and vestibular dark cells: characterisation of main structures responsible for inner-ear homeostasis, and their pathophysiological relations. *J Laryngol Otol*. 2009;123(2):151-162. doi:[10.1017/S0022215108002624](https://doi.org/10.1017/S0022215108002624)
32. Yoshida T, Naganawa S, Kobayashi M, et al. ¹⁷O-labeled water distribution in the human inner ear: insights into lymphatic dynamics and vestibular function. *Front Neurol*. 2022;13:1016577. doi:[10.3389/fneur.2022.1016577](https://doi.org/10.3389/fneur.2022.1016577)
33. Nakashima T, Naganawa S, Pyykko I, et al. Grading of endolymphatic hydrops using magnetic resonance imaging. *Acta Otolaryngol Suppl*. 2009;560:5-8. doi:[10.1080/00016480902729827](https://doi.org/10.1080/00016480902729827)

How to cite this article: Ishii M, Tanaka H, Asai R, et al. New non-contrast MRI of endolymphatic hydrops in Ménière's disease considering inversion time. *Laryngoscope Investigative Otolaryngology*. 2024;9(4):e1314. doi:[10.1002/lio2.1314](https://doi.org/10.1002/lio2.1314)